Int. J. Electrochem. Sci., 16 **(2021)** Article ID: 210452, doi: 10.20964/2021.04.36

International Journal of
ELECTROCHEMICAL
SCIENCE
www.electrochemsci.org

Transient Current of Catalytic Processes at Chemically Modified Electrodes

S. Vinolyn Sylvia[1], *R. Joy Salomi*[1], *M.E.G. Lyons*[2], *L. Rajendran*[1,*]

[1] Department of Mathematics, Academy of Maritime Education and Training(AMET) Deemed to be University, India
[2] School of Chemistry & AMBER National Centre, University of Dublin, Trinity College Dublin, Ireland
[*]E-mail: raj_sms@rediffmail.com

Received: 5 January 2021 / *Accepted:* 9 February 2021 / *Published:* 28 February 2021

The model provides reports of diffusion inside the modifier layer situated on the electrode surface of a reactant and charge carrier. This model is based on the system of strongly nonlinear equations containing the nonlinear term related to second-order chemical reaction and Michaelis-type redox reaction. In this paper, approximate analytical solutions are obtained for nonlinear equations under non-steady-state conditions using the well-established homotopy perturbation technique. Lucid and approximate polynomial expressions have been obtained for the reactant, reaction product and charge carrier concentrations and current density. The amperometric current response has been reported as a function of reactant concentration. The numerical simulation of the problem is done using a Matlab programme. The analytical results are compared with simulated data and previously published limiting cases. A reasonable agreement is observed. This paper also presents an analytical expression describing the sensitivity and response time of the biosensor electrode for all values of parameters.

Keywords: Mathematical Modeling, Nonlinear equations, Electrocatalysis, Modified electrodes, Sensitivity of biosensor.

1. INTRODUCTION

The electrocatalytic process is an important phenomenon which is widely exploited with regard to the development of biofuel cells, biosensor and electrosynthetic systems. Redox electrocatalysis within thin surface films deposited on electrode surfaces (Chemically Modified Electrodes) has been a topic of very significant worldwide interest and activity for many years. These electrodes contain an organic or inorganic thin layer, which as well as being conductive, contain active sites which can catalyse solution-phase film reactions either at the solution/film interface or inside the layer. Typical examples include the electrocatalytic reduction of hydrogen peroxide[1,2], the electro-oxidation of ascorbic

acid[3] and the electro-oxidation of some organic species at electroactive polymer modified electrodes such as for example poly(neutral red)[4], poly(toluidine blue)[5] and polyaniline[6-8], as some examples among the many electrocatalytic systems of this type so far identified.

Recently, Puida et al. [9] developed a mathematical model describing transport and electrocatalytic kinetics within surface immobilized conducting polymer modified electrodes that operate using two types of redox interaction: simple chemical second-order and a Michaelis-type adduct formation reaction. No general analytical solution for the reactant, reaction product and charge carrier concentration has been published yet, to the best of our knowledge. This communication aims to analytically solve the transient Fick reaction diffusion equations and thereby generate the analytical expressions for the reactant, reaction product and charge carrier concentration along with current for various values of pertinent parameters such as rate constant and carrier diffusion coefficient.

2. MATHEMATICAL FORMULATION OF THE PROBLEM

It is presumed that a flat electrode surface is coated by a uniform film of conducting polymer of uniform thickness *d*. The diffusion of reactant into a layer of polymer is defined by the law of the Fick.

$$\frac{\partial R(x,t)}{\partial t} = D\frac{\partial^2 R(x,t)}{\partial x^2} \quad (1)$$

where R is the concentration of reactant, t is the time, x is a space coordinate, and D is the diffusion coefficient for reactant.

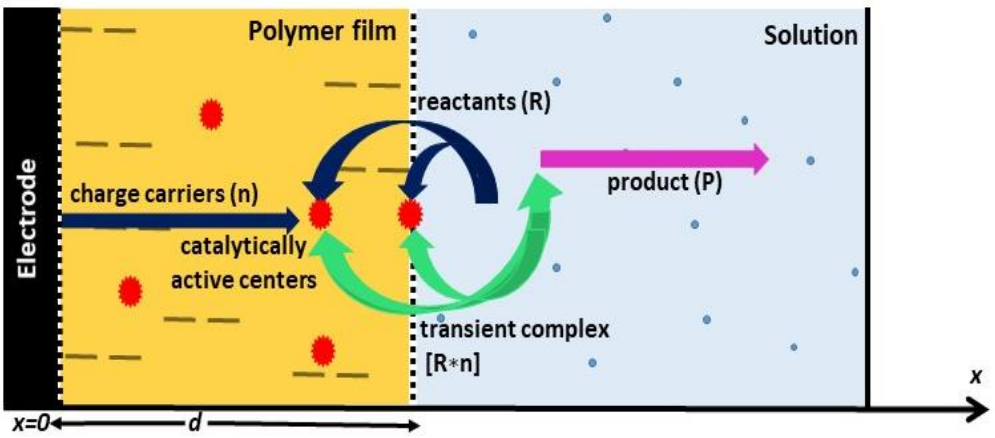

Figure 1. Schematic diagram for electrocatalysis that follows Michaelis-Menten mechanism

The electrochemical conversion (anodic oxidation or cathodic reduction) of reactants into product is influenced by the use of an appropriate electrode potential. Chemical transformation of reactant to product can either exhibit bimolecular reaction kinetics represented by the following expression [9]:

$$R + n = P \quad (2)$$

Here, R and P denote reactant and reaction product, respectively, and n is a charge carrier (electron or hole).

The pace of this reaction is defined by the kinetic rate expression:

$$\frac{dP(x,t)}{dt} = -\frac{dR(x,t)}{dt} = kR(x,t)n(x,t) \quad (3)$$

where *k* is the second-order chemical reaction rate constant. The second conversion of *R* to *P* proceeds according to the Michaelis–Menten type mechanism, that involves the formation of an adduct complex of *R* with active centres (such as polarons) carrying electric charges, followed by the decomposition of the adduct to form product *P* with regeneration of the active site. The schematic representation is given in Figure1.

$$R + n = [R * n] \quad (4)$$

$$[R * n] = P \quad (5)$$

where $[R*n]$ represents the adduct complex. The complex formation Eq. (4) in this mechanism proceeds in forward and backward directions, characterized by the rate constants k_{-1} and k_1 corresponding to forward and backward reactions, while complex break-down Eq. (5) is a one-directional process characterized by first-order catalytic rate constant k_{cat}.

In the redox processes within the porous electronically conducting polymer thin film, we assume that the polymer backbone gets oxidized then the polymer contains delocalized fixed charged sites and migrating charge carriers. Charge neutrality is accomplished by diffusing counter ions in the solution filled pores and are pinned by the fixed charged defects on the polymer chain therefore ensuring local electroneutrality. The oxidized polymer site is assumed to be catalytically active and reacts with the substrate. In so doing the product is formed and the reduced polymer site is regenerated. The reaction between reactant and oxidized polymer site will take place either within the bulk of the polymer film or in a surface reaction zone near the polymer/solution interface. Hence we can relate the carrier concentration *n* to the concentration of oxidized polymer sites. The position of the reaction zone depends on the conductivity of the polymer and its porosity.

The mass balance equations for these mechanisms can be described by the following nonlinear reaction diffusion equations for reactant (*R*), reaction product (*P*) and charge carrier (*n*) as follows [9]:

$$\frac{\partial R(x,t)}{\partial t} = D\frac{\partial^2 R(x,t)}{\partial x^2} - \alpha kR(x,t)n(x,t) - (1-\alpha)\frac{k_{cat}R(x,t)n(x,t)}{K_M + R(x,t)} \quad (6)$$

$$\frac{\partial P(x,t)}{\partial t} = D\frac{\partial^2 P(x,t)}{\partial x^2} + \alpha kR(x,t)n(x,t) + (1-\alpha)\frac{k_{cat}R(x,t)n(x,t)}{K_M + R(x,t)} \quad (7)$$

$$\frac{\partial n(x,t)}{\partial t} = D_n\frac{\partial^2 n(x,t)}{\partial x^2} - \alpha kR(x,t)n(x,t) - (1-\alpha)\frac{k_{cat}R(x,t)n(x,t)}{K_M + R(x,t)} \quad (8)$$

where $x \in [0,d]$, and $t > 0$, *d* is the polymer layer thickness. $R(x,t), P(x,t)$ and $n(x,t)$ are the reactant, reaction product and charge carrier concentrations respectively. *D* is diffusion coefficient for reactant and product, D_n is diffusion coefficient for charge carriers. α is a dimensionless coefficient, k is a second-order reaction rate constant, k_{cat} is the catalytic rate constant and K_M is the Michaelis constant. The initial conditions for Eqs. (6)-(8) are[9]

$$R(d,0) = R_0 \text{ and } R(x,0) = 0, 0 \le x < d \quad (9)$$

$$P(x,0) = 0, x \in [0,d] \quad (10)$$

$$n(x,0) = n_0, x \in [0,d] \quad (11)$$

The boundary conditions for $t > 0$ are

$$\left[\frac{\partial R}{\partial x}\right]_{x=0} = 0,\ R(d,t) = R_0, \quad (12)$$

$$\left[\frac{\partial P}{\partial x}\right]_{x=0} = 0,\ P(d,t) = 0 \quad (13)$$

$$n(0,t) = 0\,,\ \left[\frac{\partial n}{\partial x}\right]_{x=d} = 0 \tag{14}$$

The current density $I(t)$ at time *t* is defined by [9]

$$I(t) = n_e F D_n \left.\frac{\partial n(x,t)}{\partial x}\right|_{x=0} \tag{15}$$

We introduce the following dimensionless variables

$$r = \frac{R}{R_0}, p = \frac{P}{R_0}, N = \frac{n}{R_0}, X = \frac{x}{d}, T = \frac{Dt}{d^2}, k_0 = \frac{kR_0 d^2}{D}, k_1 = \frac{k_{cat} k_0}{K_M k}, \varepsilon = \frac{D_n}{D}, \beta = \frac{R_0}{K_M} \tag{16}$$

Hence Eqs. (6)-(8) can be reduced to the following dimensionless form:

$$\frac{\partial r(X,T)}{\partial T} = \frac{\partial^2 r(X,T)}{\partial X^2} - \alpha k_0 r(X,T) N(X,T) - (1-\alpha)\frac{k_1 r(X,T) N(X,T)}{1+\beta r(X,T)} \tag{17}$$

$$\frac{\partial p(X,T)}{\partial T} = \frac{\partial^2 p(X,T)}{\partial X^2} + \alpha k_0 r(X,T) N(X,T) + (1-\alpha)\frac{k_1 r(X,T) N(X,T)}{1+\beta r(X,T)} \tag{18}$$

$$\frac{\partial N(X,T)}{\partial T} = \varepsilon\frac{\partial^2 N(X,T)}{\partial X^2} - \alpha k_0 r(X,T) N(X,T) - (1-\alpha)\frac{k_1 r(X,T) N(X,T)}{1+\beta r(X,T)} \tag{19}$$

The corresponding initial and boundary conditions are [10]:

At $T = 0, r = 1, p = 0, N = \frac{n_0}{R_0}$ (20)

At $X = 0, \frac{\partial r}{\partial X} = 0, \frac{\partial p}{\partial X} = 0, N = \frac{n_0}{R_0}$ (21)

At $X = 1, r = 1, p = 0, \frac{\partial N}{\partial X} = 0$ (22)

The dimensionless current density is [10]

$$\psi(T) = \frac{I(T)d}{n_e F D_n R_0} = \left.\frac{\partial N(X,T)}{\partial X}\right|_{X=0} \tag{23}$$

3. APPROXIMATE ANALYTICAL EXPRESSION OF CONCENTRATIONS AND CURRENT UNDER NON-STEADY-STATE CONDITION USING NEW APPROACH TO HPM

Be it autocatalysis or heat exchange kinetics, numerous phenomena in engineering and the chemical sciences have been depicted using nonlinear equations. Finding solution to these nonlinear equations is of prime importance, as it helps to predict behaviour of the systems and provides an insight on the effects of parameters under consideration.

Recently some of the nonlinear equations have been solved via the use of variation iteration method (VIM) [11], the Taylor series method [12], hyperbolic functions [13], the residual method [14], the series solution technique [15], a new analytical method [16], use of the Green's function coupled with a fixed point iteration scheme [17] and the beneficial Akbari-Ganji method [18]. Among all these methods, an efficient and powerful approach for finding a solution to a system of nonlinear equations without the need for a linearization process is the homotopy perturbation method (HPM). J.H. He introduced this method for the first time in 1998 [19,20]. The HPM is a combination of the perturbation expansion and homotopy methods. This technique can take advantage of the conventional method of perturbation while eliminating its limitations, such as finding the small parameter and applying it to the equation.

In recent years many developments of this method has been presented, which have successfully solved many linear and nonlinear equations in science and engineering. Recently, K. Sayevand [21] proposed a new extension of the homotopy perturbation method, to tackle nonlinear partial differential equations (PDE) of fractional order that appear in chemical sciences. For time-dependant conditions Femila et al. [10] obtained the approximate analytical solutions for the nonlinear PDE using HPM. In his work on delay differential equations (DDE) Jameen et al. [22] introduced an approximation system algorithm for solving linear fuzzy DDE with double parametric form fuzzy numbers using HPM. B. N. Kharrat and G. A. Toma [23] proposed expanding the application of HPM that is based on Taylor series to solve nonlinear algebraic equations. Moreover, a new approach to HPM was carried out to obtain analytical expressions for transient current and concentration in redox enzymatic homogenous system for steady and non-steady-state conditions [24].

The approximate analytical expression of the dimensionless concentration of reactant (*r*), reaction product (*p*) and charge carrier (*N*) in catalytic process using a new approach to homotopy perturbation method can be obtained as follows (Appendix - A,B):

$$r(X,T) = \frac{\cosh(\sqrt{\mu_1}X)}{\cosh(\sqrt{\mu_1})} + 16\mu_1 \sum_{j=0}^{\infty} \frac{\cos\left(\frac{\pi(2j+1)X}{2}\right) e^{-\left(\frac{\pi^2(2j+1)^2}{4}+\mu_1\right)T}}{[\pi^2(2j+1)^2+4\mu_1][(2j+1)\pi]\sin\left(\frac{\pi(2j+1)}{2}\right)} \tag{24}$$

$$p(X,T) = 1 - r(X,T) \tag{25}$$

$$N(X,T) = \frac{n_0}{R_0}\left(\cosh\sqrt{\frac{\mu_2}{\varepsilon}}X - \tanh\sqrt{\frac{\mu_2}{\varepsilon}}\sinh\sqrt{\frac{\mu_2}{\varepsilon}}\,\mathrm{X}\right) + \frac{16n_0\mu_2}{R_0}\sum_{j=0}^{\infty} \frac{\cos\left(\frac{\pi(2j+1)}{2}(1-X)\right) e^{-\left(\frac{\varepsilon\pi^2(2j+1)^2}{4}+\mu_2\right)T}}{[\varepsilon\pi^2(2j+1)^2+4\mu_2][(2j+1)\varepsilon\pi]\sin\left(\frac{\pi(2j+1)}{2}\right)} \tag{26}$$

where

$$\mu_1 = \frac{\alpha k_0 n_0}{R_0} + \frac{(1-\alpha)k_1 n_0}{R_0(1+\beta)}, \mu_2 = \alpha k_0 + \frac{(1-\alpha)k_1}{(1+\beta)} \tag{27}$$

The dimensionless current using Eq. (23) is given by

$$\psi(T) = \frac{I(T)d}{n_e F D_n R_0} = \frac{n_0}{R_0}\left(\sqrt{\frac{\mu_2}{\varepsilon}}\tanh\sqrt{\frac{\mu_2}{\varepsilon}} - \frac{8\mu_2}{\varepsilon}\sum_{j=0}^{\infty}\frac{e^{-\left(\frac{\varepsilon\pi^2(2j+1)^2}{4}+\mu_2\right)T}}{[\varepsilon\pi^2(2j+1)^2+4\mu_2]}\right) \tag{28}$$

where current density *I(T)* is given by,

$$I(T) = \frac{n_e F D_n n_0}{d}\left(\sqrt{\frac{\mu_2}{\varepsilon}}\tanh\sqrt{\frac{\mu_2}{\varepsilon}} - \frac{8\mu_2}{\varepsilon}\sum_{j=0}^{\infty}\frac{e^{-\left(\frac{\varepsilon\pi^2(2j+1)^2}{4}+\mu_2\right)T}}{[\varepsilon\pi^2(2j+1)^2+4\mu_2]}\right)$$

Also from Eq. (28) and Eq. (34) we get the following equation.

$$\frac{\psi(T)}{\psi_{ss}} = 1 - \frac{8}{\varepsilon}\coth\sqrt{\frac{\mu_2}{\varepsilon}}\sum_{j=0}^{\infty}\frac{(-1)^j e^{-\left(\frac{\varepsilon\pi^2(2j+1)^2}{4}+\mu_2\right)T}}{[\varepsilon\pi^2(2j+1)^2+4\mu_2]} \tag{30}$$

4. ANALYTICAL EXPRESSION OF TIME-INDEPENDENT CONCENTRATIONS AND CURRENT

The analytical expressions of reactant (*r*), reaction product (*p*) and charge carrier (*N*) concentration in dimensionless form for steady-state condition can be obtained by applying $T \to \infty$ in Eqs. (24)-(26) as follows:

$$r_{ss}(X) = \frac{\cosh(\sqrt{\mu_1}X)}{\cosh(\sqrt{\mu_1})} \tag{31}$$

$$p_{ss}(X) = 1 - \frac{\cosh(\sqrt{\mu_1}X)}{\cosh(\sqrt{\mu_1})} \quad (32)$$

$$N_{ss}(X) = \frac{n_0}{R_0}\left(\cosh\sqrt{\frac{\mu_2}{\varepsilon}}X - \tanh\sqrt{\frac{\mu_2}{\varepsilon}}\sinh\sqrt{\frac{\mu_2}{\varepsilon}}\ \mathrm{X}\right) \quad (33)$$

The new analytical expression of steady-state current is

$$\psi_{ss} = \frac{n_0}{R_0}\sqrt{\frac{\mu_2}{\varepsilon}}\tanh\sqrt{\frac{\mu_2}{\varepsilon}} \quad (34)$$

The steady-state current density is given by

$$I_{ss} = \frac{n_e F D_n n_0}{d}\sqrt{\frac{\mu_2}{\varepsilon}}\tanh\sqrt{\frac{\mu_2}{\varepsilon}} \quad (35)$$

where $\mu_2 = \alpha k_0 + \frac{(1-\alpha)k_1}{(1+\beta)} = \frac{R_0 d^2}{D}\left(\alpha k + \frac{(1-\alpha)k_{cat}}{K_M+R_0}\right)$ (36)

The response time of the biosensor T_R is the time when the value of the absolute current slope drops below a specified small value normalised by the current value. In other terms, the time taken to attain a a specific non-dimensional rate of decay δ is used [26].

$$T_R = \min_{I(T)>0}\left\{T: \frac{1}{I(T)}\left|\frac{dI(T)}{dT}\right| < \delta\right\} \quad (37)$$

$$= \min_{I(T)>0}\left\{T: 2\left|\sum_{j=0}^{\infty}\frac{\left[\exp\left(-\left(\frac{\varepsilon\pi^2(2j+1)^2}{4}+\mu_2\right)T\right)\right]}{[\varepsilon\pi^2(2j+1)^2+4\mu_2]}\mu_2\right|\left[\sqrt{\mu_2\varepsilon}\tanh\sqrt{\frac{\mu_2}{\varepsilon}} - 8\mu_2\sum_{j=0}^{\infty}\left(\frac{\exp\left(-\left(\frac{\varepsilon\pi^2(2j+1)^2}{4}+\mu_2\right)T\right)}{[\varepsilon\pi^2(2j+1)^2+4\mu_2]}\right)\right]^{-1} < \delta\right\} \quad (38)$$

The resultant relative output signal function $I^*(T)$ can be expressed as:

$$I^*(T) = \frac{I(T_R)-I(T)}{I(T_R)} = 8\sqrt{\frac{\mu_2}{\varepsilon}}\coth\sqrt{\frac{\mu_2}{\varepsilon}}\sum_{j=0}^{\infty}\frac{e^{-\left(\frac{\varepsilon\pi^2(2j+1)^2}{4}+\mu_2\right)T}}{[\varepsilon\pi^2(2j+1)^2+4\mu_2]} \quad (39)$$

where $I(T_R) = I_{ss}$ and $I(T)$ is the output current density at time t as in Eq. (29) and I_{ss} is the steady-state current. Also, $0 \le I^*(T) < 1$ at all $T \ge 0$, $I^*(T_R) < 1$ and $I^*(T_R) = 0$.

One of the main aspects of the biosensor process is sensitivity. The dimensionless sensitivity to the reactant concentration B_s can be evaluated as follows [25]:

$$B_s(R_0) = \frac{\partial I_{ss}(R_0)}{\partial R_0} \times \frac{R_0}{I_{ss}(R_0)} \quad (40)$$

where B_s is biosensor sensitivity. Therefore from Eq. (34)

$$B_s(R_0) = \frac{[k\alpha(K_M+R_0)^2+(1-\alpha)k_{cat}K_M]\left[1+2\sqrt{\frac{\mu_2}{\varepsilon}}cosech\left(2\sqrt{\frac{\mu_2}{\varepsilon}}\right)\right]}{2(K_M+R_0)[(k\alpha(K_M+R_0)+(1-\alpha)k_{cat}]} \quad (41)$$

5. THE VALIDATION OF THE RESULTS WITH PREVIOUS LIMITING CASE RESULTS [10] AND NUMERICAL SIMULATION

Recently, Femila et al. [10] obtained approximate polynomial expressions for the current and concentration of reactant, reactant product and charge carrier in terms of diffusion coefficient and rate constant by homotopy perturbation method. On substituting $\alpha = 1$ in Eqs. (24) - (26), the concentration of reactant, reaction product and charge carrier is identical with Eqs. (18) - (21) in [10]. In addition, our current expression Eq. (34) is similar to the Eq. (25) of [10]. The system of differential equations was resolved numerically to analyse the accuracy of the solution obtained using new approach to HPM with

a finite number of terms. In Matlab software, the function pdex4 (Euler's method), which is helpful to solve boundary value problems is used to solve Eqs. (17) and (19) numerically. The comparison of analytical and numerical results is shown in Figures 2, 3 and (S1)-(S3) graphically. The comparison confirmed that our obtained analytical results were concordant with the numerical results. It can be inferred from Table 2, that the maximum percentage error deviation is 0.05.

6. RESULTS AND DISCUSSION

Eqs. (24) - (26) are the novel simplified analytic expression for concentration of the reactant, reactant product and charge carrier for all values of parameters. In Table 1, the parameter values used in [9] and in this work is given.

Table 1. Numerical values for the parameters under consideration.

Parameter	Description	Unit	Numerical value [9]	Numerical Value [This work]
k_{cat}	Catalytic rate constant	s^{-1}	1, 10, 10^2	1, 10, 50, 10^2
n_0	Concentration of charge carrier	$mol\ m^{-3}$	4×10^3	4×10^3
R_0	Concentration of reactant	$mol\ m^{-3}$	1 to 10	1 to 50
D	Diffusion coefficient for reactant and product	$m^2\ s^{-1}$	10^{-9}	10^{-9}, 1.5×10^{-9}, 2×10^{-9}, 2.5×10^{-9}
D_n	Diffusion coefficient for charge carriers	$m^2\ s^{-1}$	$10^{-11}, 10^{-10}, 10^{-9}$	$10^{-11}, 10^{-10}, 10^{-9}$, 1.5×10^{-9}, 2×10^{-9}, 2.5×10^{-9}
K_M	Michaelis constant	$mol\ m^{-3}$	5	5
k	Second-order reaction rate constant	$m^3\ mol^{-1}\ s^{-1}$	$10^{-2}, 10^{-1}, 1$	$10^{-2}, 10^{-1}$, 1,10, 50, 10^2
d	Thickness of a polymer layer	m	10^{-6}	$10^{-4}, 10^{-5}, 10^{-6}$, 1.5×10^{-6}, 2×10^{-6}, 2.5×10^{-6}, 3×10^{-6}
α	Dimensionless coefficient	none	0 to 1	0 to 1
β	Dimensionless parameter	none	0 to 2	0.1, 1, 5, 10, 10^{-2}
k_0	Dimensionless parameter	none	0 to 10^{-2}	0.1, 1, 5, 10, 10^{-2}
k_1	Dimensionless parameter	none	0 to 0.2	0.1, 1, 5, 10, 10^{-2}

Table 2. Comparison of dimensionless concentration of reactant (r), reaction product (p) and charge carrier (N) with simulation results for $\beta = 0.5, k_0 = 10, k_1 = 0.1, T = 1$.

X	Concentration of reactant (r)			Concentration of reaction product (p)			Concentration of charge carrier (N)		
	$\alpha = 0.1$			$\alpha = 0.1$			$\alpha = 0.5$		
	Numerical	Analytical Eq. (24)	% of deviation	Numerical	Analytical Eq. (25)	% of deviation	Numerical	Analytical Eq. (26)	% of deviation
0	0.6447	0.6448	0.02	0.3553	0.3552	0.03	1	1	0.00

0.1	0.6480	0.6480	0.00	0.352	0.352	0.00	0.7962	0.7961	0.01
0.2	0.6577	0.6577	0.00	0.3423	0.3423	0.00	0.6359	0.6359	0.00
0.3	0.6740	0.6740	0.00	0.326	0.326	0.00	0.5105	0.5105	0.00
0.4	0.6971	0.6971	0.00	0.3029	0.3029	0.00	0.4131	0.4131	0.00
0.5	0.7273	0.7273	0.00	0.2727	0.2727	0.00	0.3383	0.3382	0.03
0.6	0.7650	0.7649	0.01	0.235	0.2351	0.04	0.2820	0.2819	0.04
0.7	0.8105	0.8104	0.01	0.1895	0.1896	0.05	0.2411	0.2410	0.04
0.8	0.8645	0.8643	0.02	0.1355	0.1357	0.15	0.2134	0.2133	0.05
0.9	0.9275	0.9273	0.02	0.0725	0.0727	0.28	0.1973	0.1973	0.00
1	1	1	0.00	0	0	0	0.1921	0.1921	0.00

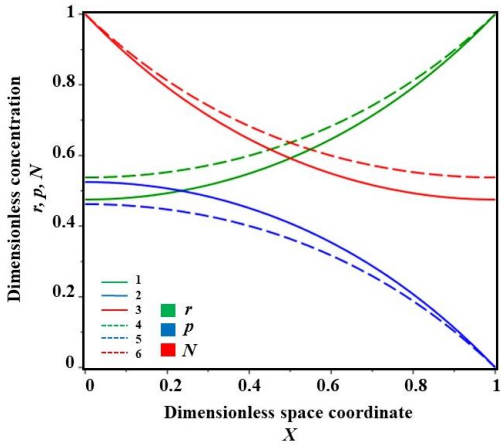

Figure 2. Profiles of dimensionless concentrations of the reactant (1,4), reaction product (2,5) and charge carrier (3,6) along the polymer film at steady-state. Solid line represents time T = 5 and dotted line represents T = 0.5. The numerical values of other parameters are $\alpha = 0.1, \beta = 100, k_0 = 10, k_1 = 100, \xi = 1, r_0 = 1$ and $N_0 = 1$.

Figure 2 represents the steady-state concentration of reactant *r*, reaction product *p* and charge carrier *N* respectively. From the same figure, it can be noted that the concentration of reactant *r* and reaction product *p* are increasing functions whereas the charge carrier *N* is a decreasing function from the film/solution interface to the electrode.

Figure S1 shows that, the concentration of reactant *r* increases with a fall in k_0 and k_1 values and it reaches the steady-state for $k_0, k_1 \geq 100$. The reactant concentration *r* is directly proportional to β, also when $\beta \geq 1000$ this concentration becomes uniform. As α increases from 0 to 1, *r* increases. Figure S1 and Figure S2 indicate that the influence of the parameters k_0, k_1, α and β on reaction product concentration *p* and reactant concentration *r* are inversely proportional.

In Figure S3, the concentration of charge carriers *N* varies inversely with k_0 and k_1, while α (dimensionless coefficient) and β (dimensionless parameter) are directly proportional to *N*. Here the concentration of charge carriers *N* is uniform when β is greater than 100.

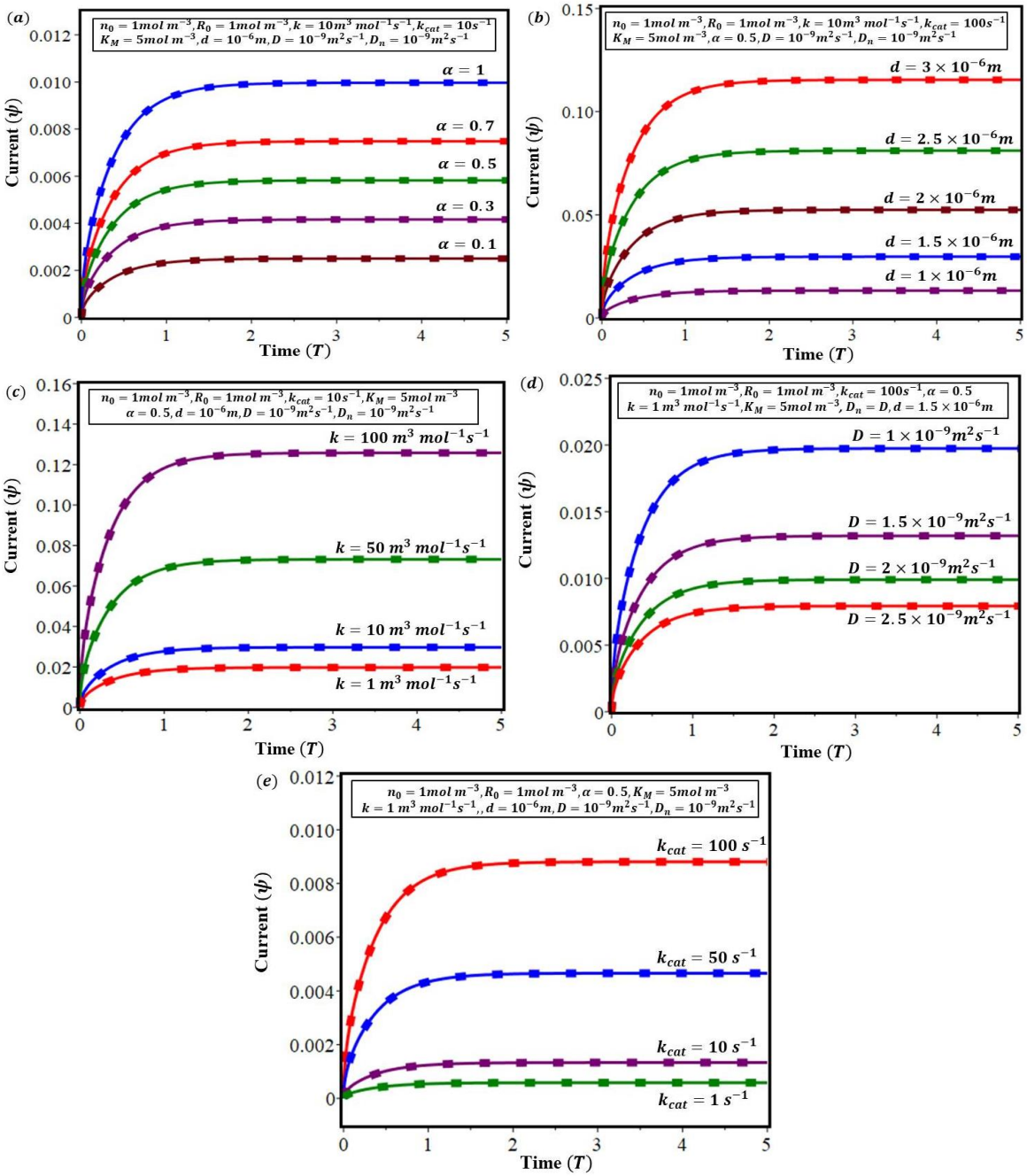

Figure 3. Current versus time for various values of (a) dimensionless coefficient α, (b) thickness of polymer layer d, (c) second-order reaction rate constant k, (d) Diffusion coefficient D and (e) catalytic rate constant k_{cat} Eq. (28). Solid line represents numerical results and dotted line represents analytical results.

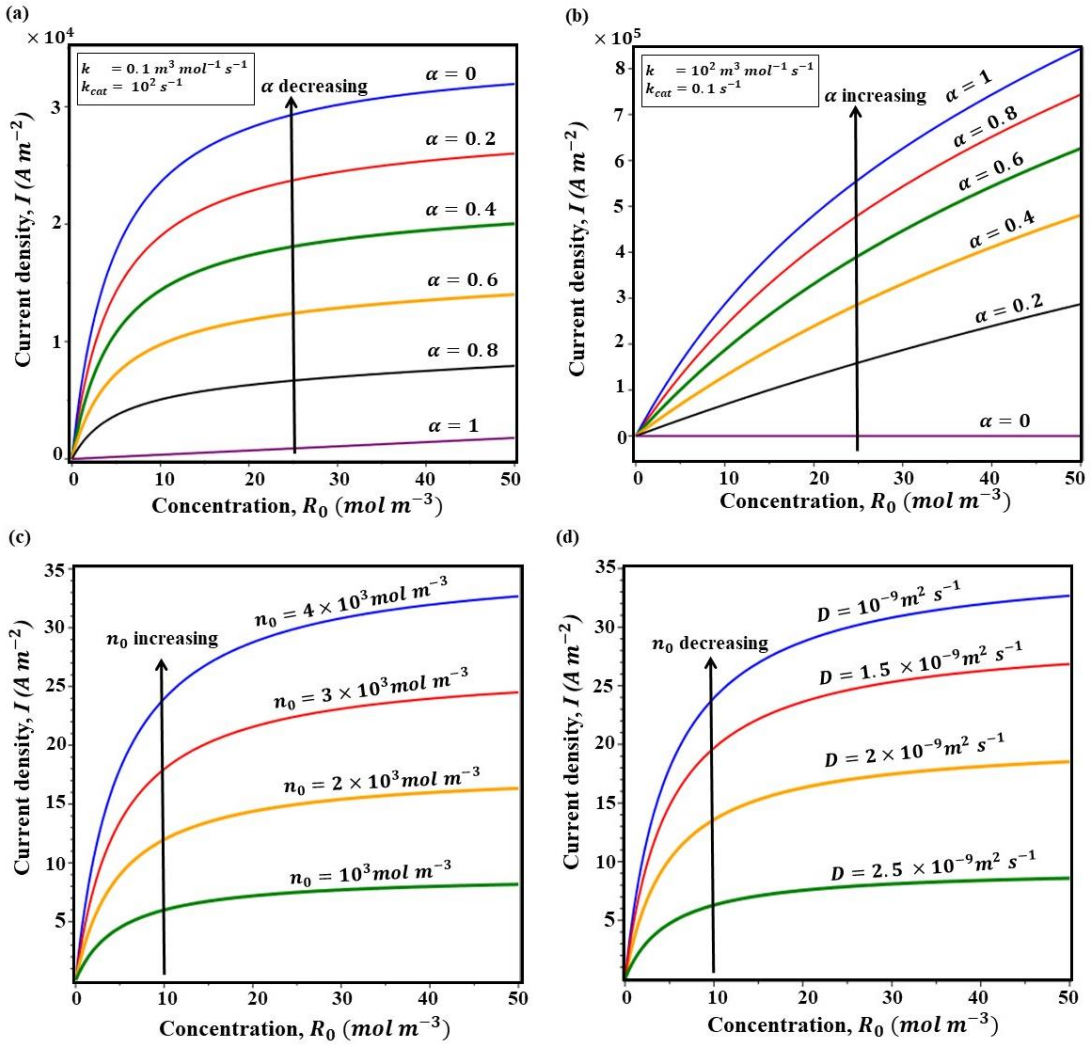

Figure 4. Current I Eq. (29) versus initial concentration of reactant R_0 for different parameter values. The common fixed values of the parameters [9] are $D = 10^{-9} m^2\ s^{-1}, K_M = 5\ mol\ m^{-3}, d = 10^{-6} m$

(a) $n_0 = 4 \times 10^3 mol\ m^{-3}, k_{cat} = 10^2\ s^{-1}, k = 0.1 m^3\ mol^{-1}\ s^{-1},\ t = 0.001\ s,\ D_n = 10^{-9} m^2\ s^{-1}$.

(b) $n_0 = 4 \times 10^3 mol\ m^{-3}, k_{cat} = 0.1\ s^{-1}, k = 10^2 m^3\ mol^{-1}\ s^{-1},\ t = 0.001\ s,\ D_n = 10^{-9} m^2\ s^{-1}$.

(c) $\alpha = 0, k_{cat} = 0.1\ s^{-1}, k = 1 m^3\ mol^{-1}\ s^{-1}, D_n = 10^{-9} m^2\ s^{-1}, t = 0.001\ s$.

(d) $\alpha = 0, k_{cat} = 0.1\ s^{-1}, k = 1 m^3\ mol^{-1}\ s^{-1}, n_0 = 4 \times 10^3 mol\ m^{-3}$.

Figure 3 signifies that as $T \to 1$, the current becomes stable for all values of experimental parameters. Also it can be established that, current is directly proportional to thickness of the polymer film *d.* An increase in the parameters k_{cat}, k and α leads to an increase in current. However, the diffusion coefficient *D* varies inversely with current.

Figures 4 (a) and (b) represents current versus reactant concentration for various value of k_{cat}, k and α. It can be noted that the current response to concentration rises, at increasing α for $k > 0.1 k_{cat}$ $m^3\ mol^{-1}$or decreasing α for $k < 0.1 k_{cat}\ m^3\ mol^{-1}$. From Figures 4 (a) and (b) it is also observed that

the concentration-current curve is linear when $\frac{k_1}{k_0} = \frac{k_{cat}}{K_M k}$ is large and $\alpha = 1$, The caliberation curve of reactant concentration versus current is a straight line when $\frac{k_1}{k_0} = \frac{k_{cat}}{K_M k}$ is very small corresponding to $\alpha = 0$.

Figures 4 (c) and (d) represent the concentration-current (hyperbolic) curves for pure Michaelis-Menten mechanism, corresponding to $\alpha = 0$. Indeed, an increase of n_0 means a progressive increase of current and same is observed with a decrease of D. The electron transition range is enhanced due to increase of concentration of charge carrier n_0 and R_0 this inturn increases current.

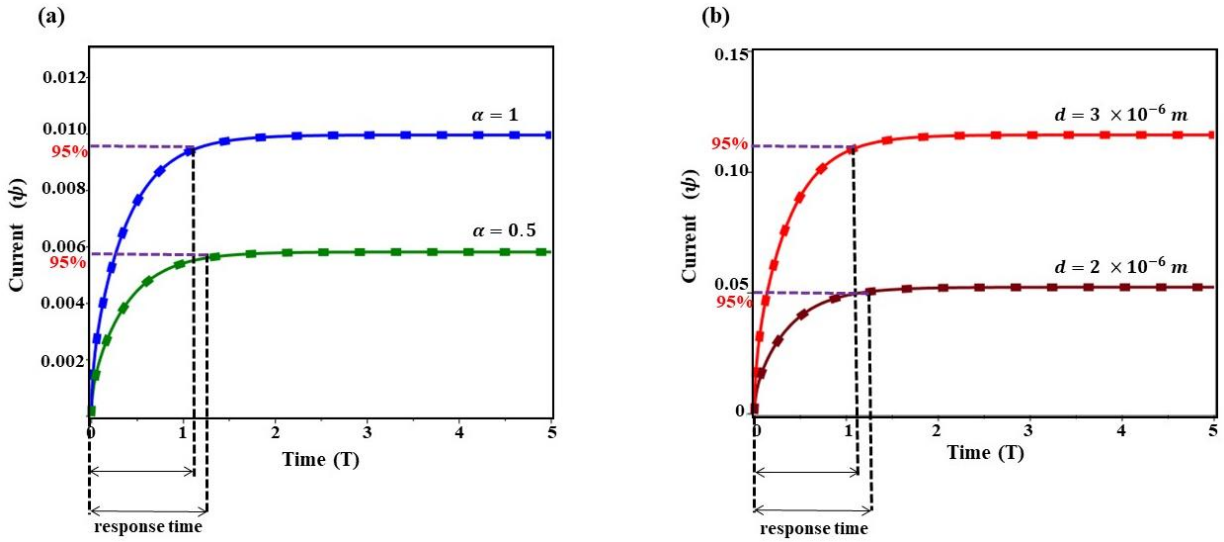

Figure 5. The reponse time graph with variation in α (a) and polymer film thickness d (b).
Response time is the time for having 95% of the response or it can be defined as the time taken by the sensors to give a fixed value for the minimum amount of analyte.

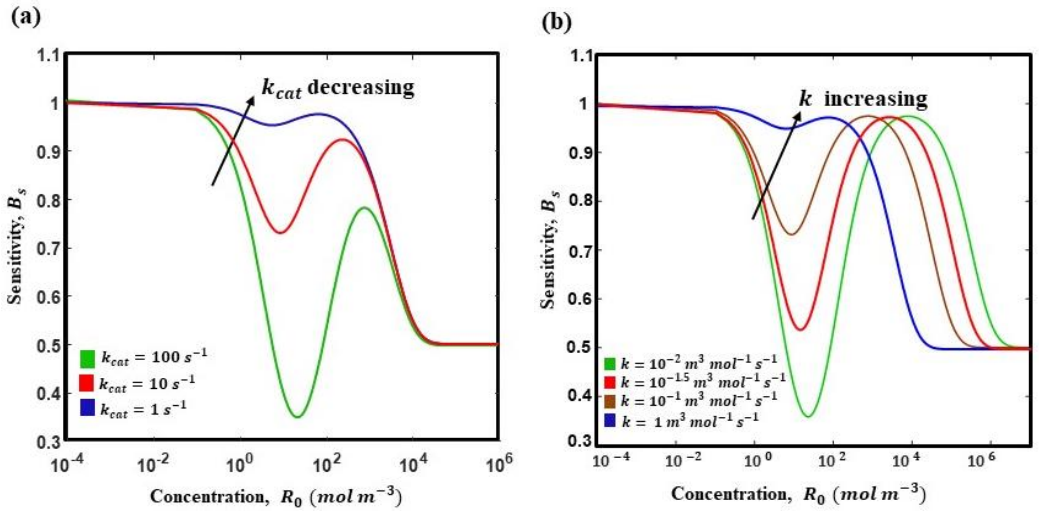

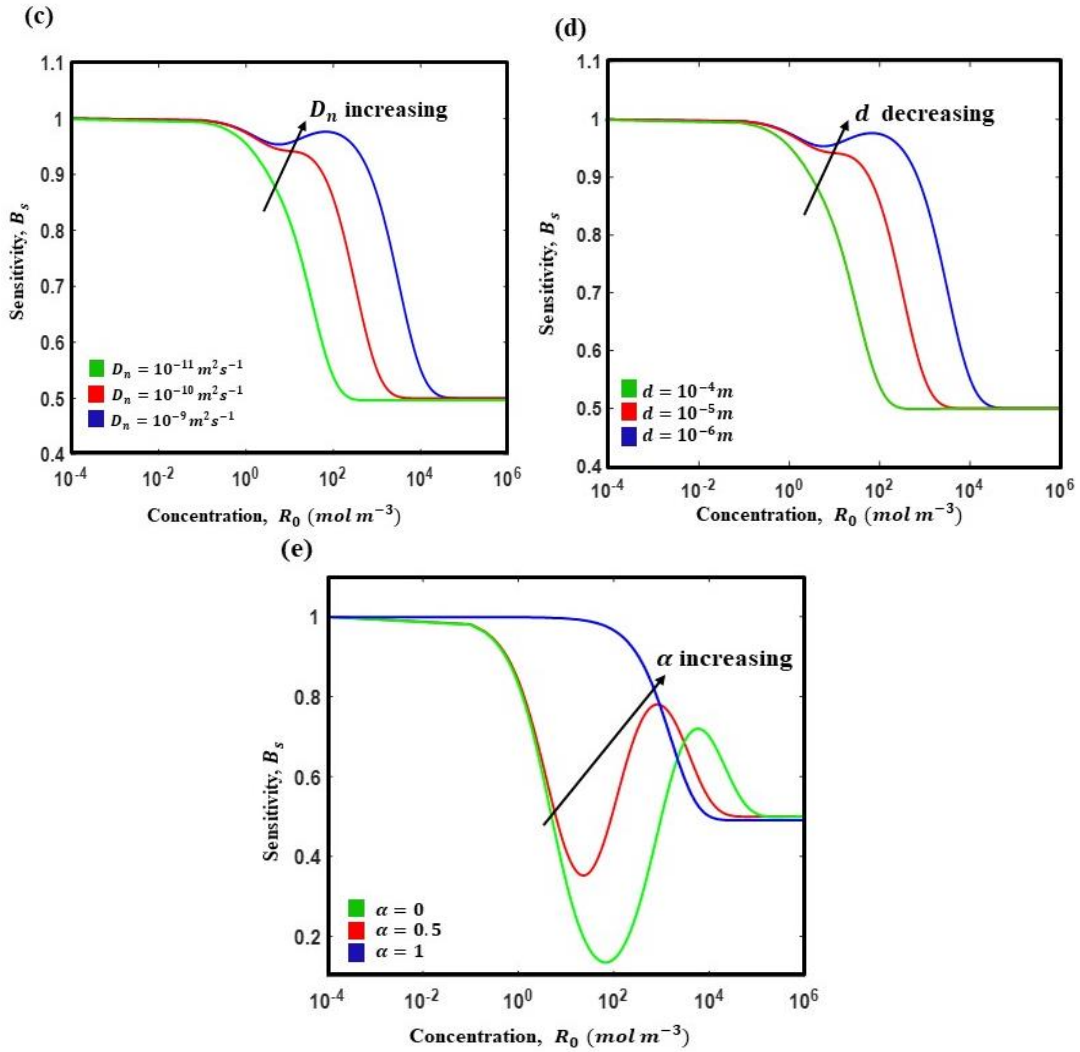

Figure 6. Sensitivity of biosensor B_s Eq. (41) versus initial concentration of reactant R_0 for various values parameters. The common fixed values of the parameters are $n_0 = 4 \times 10^3 mol\, m^{-3}$, $K_M = 5\, mol\, m^{-3}$.

(a) $D_n = D = 10^{-9} m^2\, s^{-1}, k = 1\, m^3\, mol^{-1}\, s^{-1}, \alpha = 0.5, d = 10^{-6} m$

(b) $D_n = D = 10^{-9} m^2\, s^{-1}, k_{cat} = 1\, s^{-1}, \alpha = 0.5, d = 10^{-6} m$

(c) $D = 10^{-9} m^2\, s^{-1}, k = 1\, m^3\, mol^{-1}\, s^{-1}, k_{cat} = 1\, s^{-1}, \alpha = 0.5, d = 10^{-6} m$

(d) $D_n = D = 10^{-9} m^2\, s^{-1}, k = 1\, m^3\, mol^{-1}\, s^{-1}, k_{cat} = 1\, s^{-1}, \alpha = 0.5$

(e) $D_n = D = 10^{-9} m^2\, s^{-1}, k = 1 m^3\, mol^{-1}\, s^{-1}, k_{cat} = 100\, s^{-1}$

From Figure 5 it can be inferred that a decrease in thickness of polymer film, prolongs the response time. For higher α value or as the reaction follows a simple redox process, the response time is reduced. Here the overall response time is less than 2 *s* for all values of other parameters.

Figures 6. (a)–(e) depicts a non-monotonic biosensor sentivity B_s. When the initial concentration of reactant R_0 is small, B_s reaches the value 1. Sensitivity attains the steady-state value of 0.5, when the initial concentration of reactant is very large. One can see from the figures that the shape of all the curves of sensitivity is similar.

An increase in second order reaction rate k, increases the biosensor sensitivity B_s, however same effect on B_s is observed for decreasing values of catalytic rate constant k_{cat}. A fall in sensitivity B_s can be noted, for increasing thickness of the polymer film d. When $d \leq 10^{-6}\, m$ sensitivity has negligible

increment and maintains the same curve. Moreover, as the reaction follows a Michaelis-Menten type of mechanism $\alpha = 0$, a decrease in sensitivity B_s is registered. With a rise of charge carrier diffusion coefficient D_n, sensitivity rises evidently. The linear range of the biosensor sensitivity calibration curve over R_0 is observed whenever $R_0 < 1\ mol\ m^{-3}$ for all other parameters values.

7. CONCLUSION

An essential mathematical study of the diffusion of reactant and charge carriers inside the modifier layer situated at the electrode surface and the redox interaction between the reactant and the active centre bearing charge carriers has been reported. By resolving the nonlinear reaction-diffusion equation using the new approach to the homotopy perturbation method, an approximate analytical expression of reactant, reaction product and charge carrier concentration and current is obtained. Analytical results are compared with simulation results. The effect of electrocatalytic parameters on the sensitivity of biosensors has been noted. Such analytical results are helpful in predicting and optimising the kinetic parameters of modified electrodes.

DECLARATION OF COMPETING INTEREST
The authors declare that they have no known competing financial interests or personal relationships that could have appeared to influence the work reported in this paper.

ACKNOWLEDGEMENT
The authors are grateful to Shri J.Ramachandran, Chancellor and Col.Dr.G.Thiruvasagam, Vice-Chancellor, Academy of Maritime Education and Training (AMET), Chennai, Tamil Nadu for their encouragement. They are also thankful to the reviewers for their comments.

APPENDIX-A. Approximate analytical solution of the nonlinear Eqs. (17) and (19) using the new approach to HPM

In this Appendix, we stated how to evaluate the solution of Eq. (17) using boundary conditions Eqs. (20)-(22). The homotopy to solve Eq. (17) can be constructed as follows:

$$(1-l)\left[\frac{\partial r}{\partial T}-\frac{\partial^2 r}{\partial X^2}+\alpha k_0 rN(T=0)+(1-\alpha)\frac{k_1 rN(T=0)}{1+\beta r(T=0)}\right]+l\left[\frac{\partial r}{\partial T}-\frac{\partial^2 r}{\partial X^2}+\alpha k_0 rN+(1-\alpha)\frac{k_1 rN}{1+\beta r}\right]=0 \quad (A.1)$$

(or)

$$(1-l)\left[\frac{\partial r}{\partial T}-\frac{\partial^2 r}{\partial X^2}+\frac{\alpha k_0 n_0 r}{R_0}+(1-\alpha)\frac{k_1 n_0 r}{R_0(1+\beta)}\right]+l\left[\frac{\partial r}{\partial T}-\frac{\partial^2 r}{\partial X^2}+\alpha k_0 rN+(1-\alpha)\frac{k_1 rN}{1+\beta r}\right]=0 \quad (A.2)$$

The initial and boundary conditions are

$$\text{At } T=0, r=1, \text{At } X=0, \frac{\partial r}{\partial X}=0, \text{At } X=1, r=1 \quad (A.3)$$

The approximate solution of Eq. (A.2) is

$$r = r_0 + l r_1 + l^2 r_2 + \cdots \quad (A.4)$$

Substituting Eq. (A.4) into Eq. (A.2) and arranging the coefficients of powers l, we get

$$l^0 : \frac{\partial r_0}{\partial T}-\frac{\partial^2 r_0}{\partial X^2}+\mu_1 r_0 = 0 \quad (A.5)$$

$$\text{where } \mu_1 = \frac{\alpha k_0 n_0}{R_0}+\frac{(1-\alpha)k_1 n_0}{R_0(1+\beta)} \quad (A.6)$$

The initial and boundary conditions for Eq. (A.5) becomes

$$\text{At } T=0, r_0=1, \text{At } X=0, \frac{\partial r_0}{\partial X}=0, \text{At } X=1, r_0=1 \quad (A.7)$$

In the Laplace plane, the PDE Eq. (A.5) and the corresponding boundary conditions Eq.(A.7) become as follows:

$$\frac{d^2\bar{r}_0}{dX^2} - (s+\mu_1)\bar{r}_0 + 1 = 0 \tag{A.8}$$

The corresponding boundary conditions are

$$\text{At } X = 0, \frac{\partial \bar{r}_0}{\partial X} = 0, \text{ At } X = 1, \bar{r}_0 = 1/s \tag{A.9}$$

where s is the Laplace variable and $\bar{r}_0$ is the Laplace transformed variable of r_0.

Using the boundary conditions Eq. (A.9), we can get the following solution of Eq. (A.8) as

$$\bar{r}_0(X) = \frac{1}{s+\mu_1} + \frac{\mu_1}{s(s+\mu_1)} \frac{\cosh(\sqrt{s+\mu_1}X)}{\cosh(\sqrt{s+\mu_1})} \tag{A.10}$$

By means of complex inversion formula

$$r_0(X,T) = \frac{1}{2\pi i}\int_{\gamma-i\infty}^{\gamma+i\infty} e^{sT}\,\bar{r}_0(X,s)ds = \text{sum of the contributions from all the poles of the integrand.} \tag{A.11}$$

$$\text{Res}\left(\frac{e^{sT}}{s+\mu_1}\right) = e^{-\mu_1 T} \tag{A.12}$$

Hence, in order to invert Eq. (A.10), we need to evaluate

$$\text{Res}\left[\frac{\mu_1 e^{sT}}{s(s+\mu_1)} \frac{\cosh(\sqrt{s+\mu_1}X)}{\cosh(\sqrt{s+\mu_1})}\right] \tag{A.13}$$

There is a simple pole at $s = 0$ and $s = -\mu_1$. Also, there are infinitely many poles given by the solution of the equation $\cosh(\sqrt{s+\mu_1}) = 0$ and they are $s_j = -\frac{(2j+1)^2\pi^2}{4} - \mu_1$ where $j = 0,1,2, \ldots$

Hence

$$\begin{aligned}\text{Res}\left[\frac{\mu_1 e^{sT}}{s(s+\mu_1)} \frac{\cosh(\sqrt{s+\mu_1}X)}{\cosh(\sqrt{s+\mu_1})}\right] =& \text{Res}\left[\frac{\mu_1 e^{sT}}{s(s+\mu_1)} \frac{\cosh(\sqrt{s+\mu_1}X)}{\cosh(\sqrt{s+\mu_1})}\right]_{s=0} + \text{Res}\left[\frac{\mu_1 e^{sT}}{s(s+\mu_1)} \frac{\cosh(\sqrt{s+\mu_1}X)}{\cosh(\sqrt{s+\mu_1})}\right]_{s=-\mu_1} \\ &+ \text{Res}\left[\frac{\mu_1 e^{sT}}{s(s+\mu_1)} \frac{\cosh(\sqrt{s+\mu_1}X)}{\cosh(\sqrt{s+\mu_1})}\right]_{s=s_j}\end{aligned} \tag{A.14}$$

The residue at $s = 0$ is given by

$$\text{Res}\left[\frac{\mu_1 e^{sT}}{s(s+\mu_1)} \frac{\cosh(\sqrt{s+\mu_1}X)}{\cosh(\sqrt{s+\mu_1})}\right]_{s=0} = \lim_{s\to 0}\left[\frac{(s-0)\mu_1 e^{sT}}{s(s+\mu_1)} \frac{\cosh(\sqrt{s+\mu_1}X)}{\cosh(\sqrt{s+\mu_1})}\right] = \frac{\cosh(\sqrt{\mu_1}X)}{\cosh(\sqrt{\mu_1})} \tag{A.15}$$

The residue at $s = -\mu_1$ is given by

$$\text{Res}\left[\frac{\mu_1 e^{sT}}{s(s+\mu_1)} \frac{\cosh(\sqrt{s+\mu_1}X)}{\cosh(\sqrt{s+\mu_1})}\right]_{s=-\mu_1} = \lim_{s\to -\mu_1}\left[\frac{(s+\mu_1)\mu_1 e^{sT}}{s(s+\mu_1)} \frac{\cosh(\sqrt{s+\mu_1}X)}{\cosh(\sqrt{s+\mu_1})}\right] = -e^{-\mu_1 T} \tag{A.16}$$

The residue at $s = s_j$ is given by

$$\begin{aligned}\text{Res}\left[\frac{\mu_1 e^{sT}}{s(s+\mu_1)} \frac{\cosh(\sqrt{s+\mu_1}X)}{\cosh(\sqrt{s+\mu_1})}\right]_{s=s_j} &= \lim_{s\to s_j}\left[\frac{\mu_1 e^{sT}}{s(s+\mu_1)} \frac{\cosh(\sqrt{s+\mu_1}X)}{\frac{d}{ds}\cosh(\sqrt{s+\mu_1})}\right] \\ &= 16\mu_1 \sum_{j=0}^{\infty} \frac{e^{-\left(\frac{\pi^2(2j+1)^2}{4}+\mu_1\right)T} \cos\left(\frac{(2j+1)\pi X}{2}\right)}{[\pi^2(2j+1)^2+4\mu_1](2j+1)\pi \sin\left(\frac{(2j+1)\pi}{2}\right)}\end{aligned} \tag{A.17}$$

From Eqs. (A.10) - (A.17) we get Eq. (24) in the text. Similarly, using complex inversion formula we can solve Eq. (19).

APPENDIX-B. Relation between $r(X,T)$ & $p(X,T)$

On adding Eq. (17) and Eq. (18), we get

$$\frac{\partial[r(X,T)+p(X,T)]}{\partial T} = \frac{\partial^2[r(X,T)+p(X,T)]}{\partial X^2} \tag{B.1}$$

If $f(X,T) = r(X,T) + p(X,T)$, then Eq. (B.1) becomes

$$\frac{\partial f(X,T)}{\partial T} = \frac{\partial^2 f(X,T)}{\partial X^2} \tag{B.2}$$

The corresponding initial and boundary conditions are

$$\text{At } T = 0, f = 1, \text{ At } X = 0, \frac{\partial f}{\partial X} = 0, \text{ At } X = 1, f = 1 \tag{B.3}$$

In the Laplace plane, the PDE Eq. (B.2) and the corresponding boundary conditions Eq. (B.3) become as follows:

$$\frac{d^2\bar{f}}{dX^2} - s\bar{f} + 1 = 0 \quad \text{(B.4)}$$

The corresponding boundary conditions are

$$\text{At } X = 0, \frac{\partial \bar{f}}{\partial X} = 0, \text{ At } X = 1, \bar{f} = 1/s \quad \text{(B.5)}$$

On solving Eq. (B.4) using Eq. (B.5), we get

$$\bar{f}(X, s) = \frac{1}{s} \quad \text{(B.6)}$$

Taking inverse Laplace transform of Eq. (B.6) we obtain

$$f(X, T) = 1 \quad \text{(B.7)}$$

$$\text{Thus, } p(X, T) = 1 - r(X, T) \quad \text{(B.8)}$$

NOMENCLATURE

Symbol	Description	Unit
R	Concentration of reactant	$mol\ m^{-3}$
P	Concentration of reaction product	$mol\ m^{-3}$
n	Concentration of charge carrier	$mol\ m^{-3}$
k_{cat}	Catalytic rate constant	s^{-1}
I	Density of the current	$A\ m^{-2}$
D	Diffusion coefficient for reactant and product	$m^2\ s^{-1}$
D_n	Diffusion coefficient for charge carriers	$m^2\ s^{-1}$
x	Distance from electrode	m
F	Faraday's constant	$C\ mol^{-1}$
R_0	Initial concentration of reactant $(x = d)$	$mol\ m^{-3}$
n_0	Initial concentration of charge carrier	$mol\ m^{-3}$
K_M	Michaelis constant	$mol\ m^{-3}$
k	Second-order reaction rate constant	$m^3\ mol^{-1}\ s^{-1}$
d	Thickness of a polymer layer	m
t	Time	s
α	Dimensionless coefficient	*None*
r	Dimensionless concentration of reactant	*None*
p	Dimensionless concentration of reaction product	*None*
N	Dimensionless concentration of charge carrier	*None*
r_{ss}	Dimensionless concentration of reactant at steady-state	*None*
p_{ss}	Dimensionless concentration of reaction product at steady-state	*None*
N_{ss}	Dimensionless concentration of charge carrier at steady-state	*None*
ψ	Dimensionless current	*None*
ψ_{ss}	Dimensionless current at steady-state	*None*
X	Dimensionless distance from electrode	*None*
δ	Dimensionless decay rate	*None*
k_0	Dimensionless parameter	*None*
k_1	Dimensionless parameter	*None*
β	Dimensionless parameter	*None*
T	Dimensionless time	*None*
n_e	Number of electrons	*None*
ε	Ratio of diffusion coefficient	*None*

References

1. R. Mazeikiene, G. Niaura, A. Malinauskas, *J. Electroanal. Chem.,* 660(1) (2011) 140–146.
2. R. Araminaite, R. Garjonyte, A. Malinauskas, *J. Solid State Electrochem.,* 14(1) (2010) 149–155.
3. R. Araminaite, R. Garjonyte, A. Malinauskas, *Cent. Eur. J. Chem.,* 7(4) (2009) 739-744.
4. R. Mazeikiene, K. Balskus, O. Eicher-Lorka, G. Niaura, R. Meskys, A. Malinauskas, *Vibrat. Spectrosc.,* 51(2) (2009) 238–247.
5. R. Mazeikiene, G. Niaura, A. Malinauskas, *Electrochim. Acta*, 53(26) (2008) 7736–7743.
6. K. Brazdziuviene, I. Jureviciute, A. Malinauskas, *Electrochim. Acta,* 53(2) (2007) 785–791.
7. R. Mazeikiene, G. Niaura, A. Malinauskas, *Electrochim. Acta,* 51(26) (2006) 5761–5766.
8. R. Mazeikiene, G. Niaura, A. Malinauskas, *Electrochem. Commun.,* 7(10) (2005)1021–1026.
9. M. Puida, A. Malinauskas, F. Ivanauskas, *J. Math. Chem.,* 50(7) (2012) 2001–2011.
10. J. Femila Mercy Rani, T. Iswarya, L. Rajendran, *Quim. Nova,* 40(8) (2017) 880-884.
11. A. M. Wazwaz, *Optik*, 207 (2020) 164457.
12. R. Usha Rani, L. Rajendran, *Chem. Phys. Lett*. 754 (2020) 137573.
13. K. Nirmala, B. Manimegalai, L. Rajendran, *Int. J. Electrochem. Sci.* 15 (2020) 5682 – 5697.
14. K. Saranya, V. Mohan, L. Rajendran, *J. Math. Chem.* 58 (2020) 1230-1246.
15. R. Joy Salomi, S. Vinolyn Sylvia, L. Rajendran, M. Abukhaled, *Sens. Actuators B Chem*., 321 (2020) 128576.
16. J. Visuvasam, A. Meena, L. Rajendran, *J. Electroanal. Chem.,* 869 (2020) 114106.
17. M. Abukhaled, S.A. Khuri, *J. Electroanal. Chem.,* 792 (2017) 66–71.
18. M.E.G. Lyons, *J Solid State Electrochem.,* 24 (2020) 2751–2761.
19. J.H. He, *Comput. Methods. Appl. Mech. Eng.,* 178(3-4) (1999) 257-262.
20. J.H. He, *Internat. J. Non-Linear Mech.,* 35(1) (2000) 37-43.
21. K. Sayevand, *J. Math. Chem.,* 58 (2020) 1291–1305.
22. A. F. Jameel, S. G. Amen, A. Saaban, N. H. Man, F. M. Alipiah, *Mathematics and Statistics,* 8(5) (2020) 551-558.
23. B. N. Kharrat, G. A. Toma, *Int. J. Sci. Res. Math. Stat. Sci.,* 7(2) (2020) 47-50.
24. M. Rasi, L. Rajendran, A. Subbiah, *Sens. Actuators B Chem.,* 208 (2015) 128–136.
25. R. Baronas, J. Kulys, K. Petrauskas, J. Razumiene, *Sensors,* 12 (2012) 9146-9160.
26. R. Baronas, F. Ivanauskas, & J. Kulys, *Sensors,* 3(7) (2003) 248–262.

SUPPLEMENTARY MATERIAL

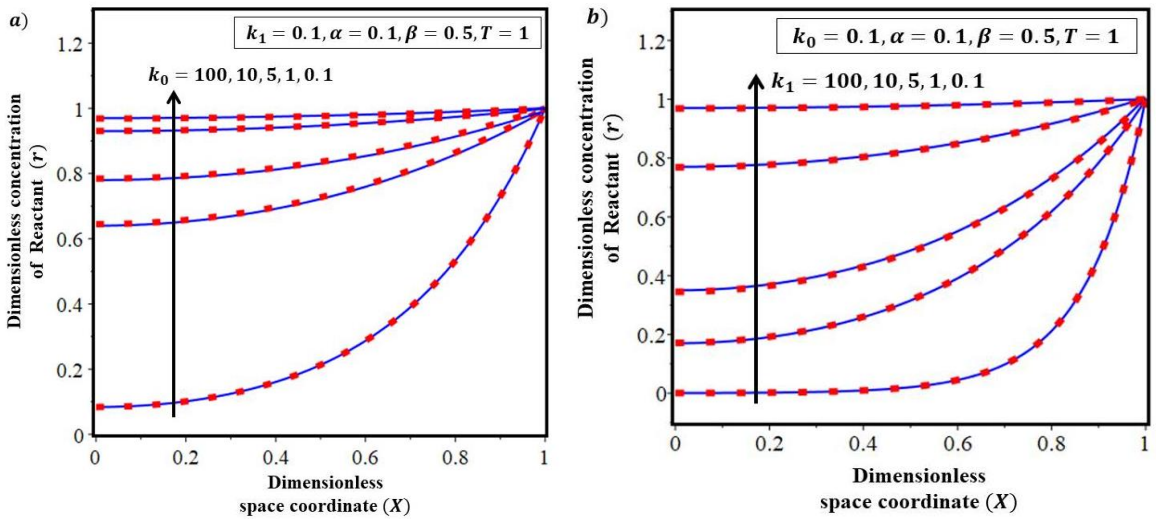

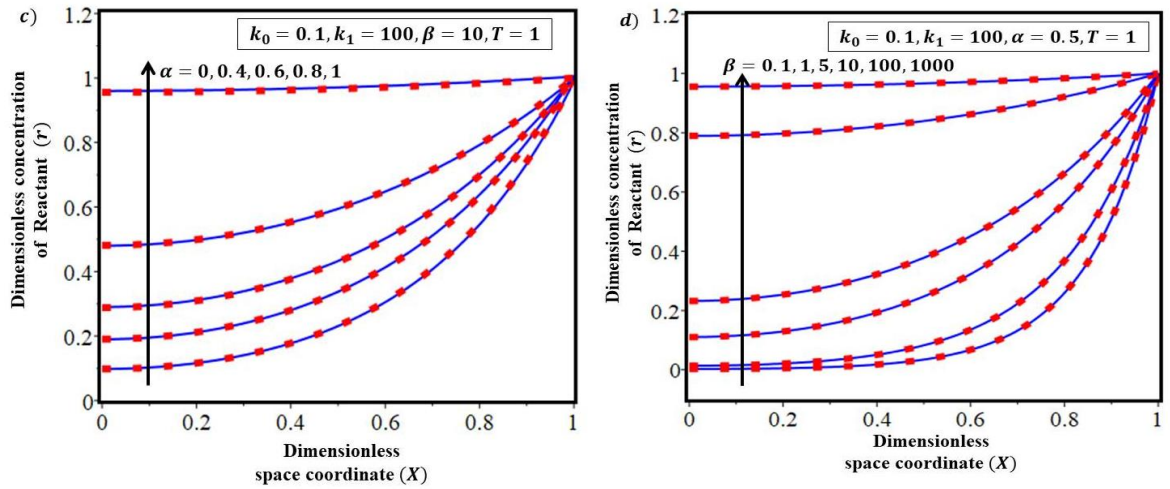

Figure S1. Comparison between analytical (dotted) and numerical (solid) results for the dimensionless concentration of reactant (r) against the dimensionless space coordinate (X) for various values of the parameters (Eq. (24)).

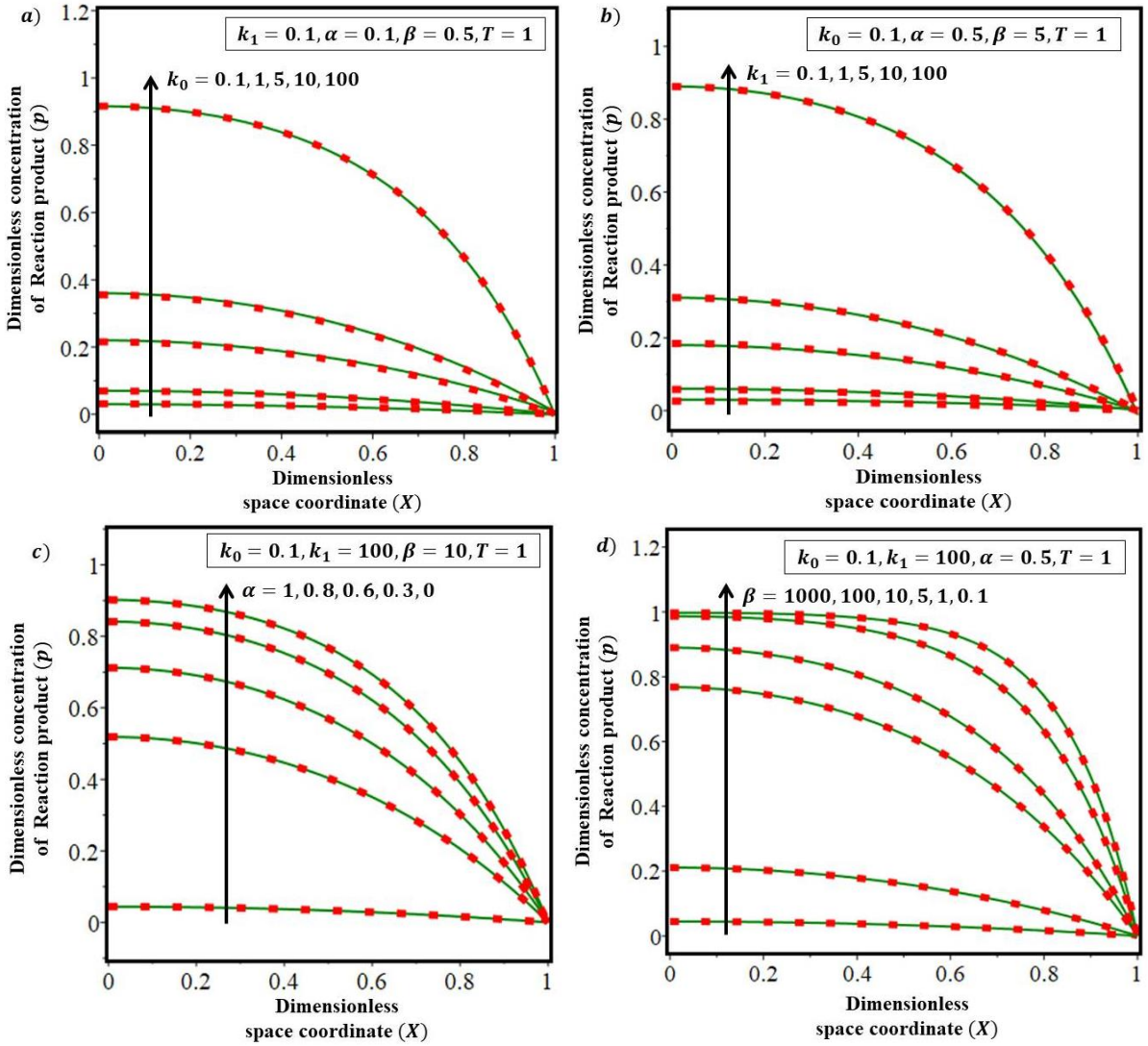

Figure S2. Comparison between analytical (dotted) and numerical (solid) results for the dimensionless concentration of reaction product (p) against the dimensionless space coordinate (X) for various values of the parameters (Eq. (25)).

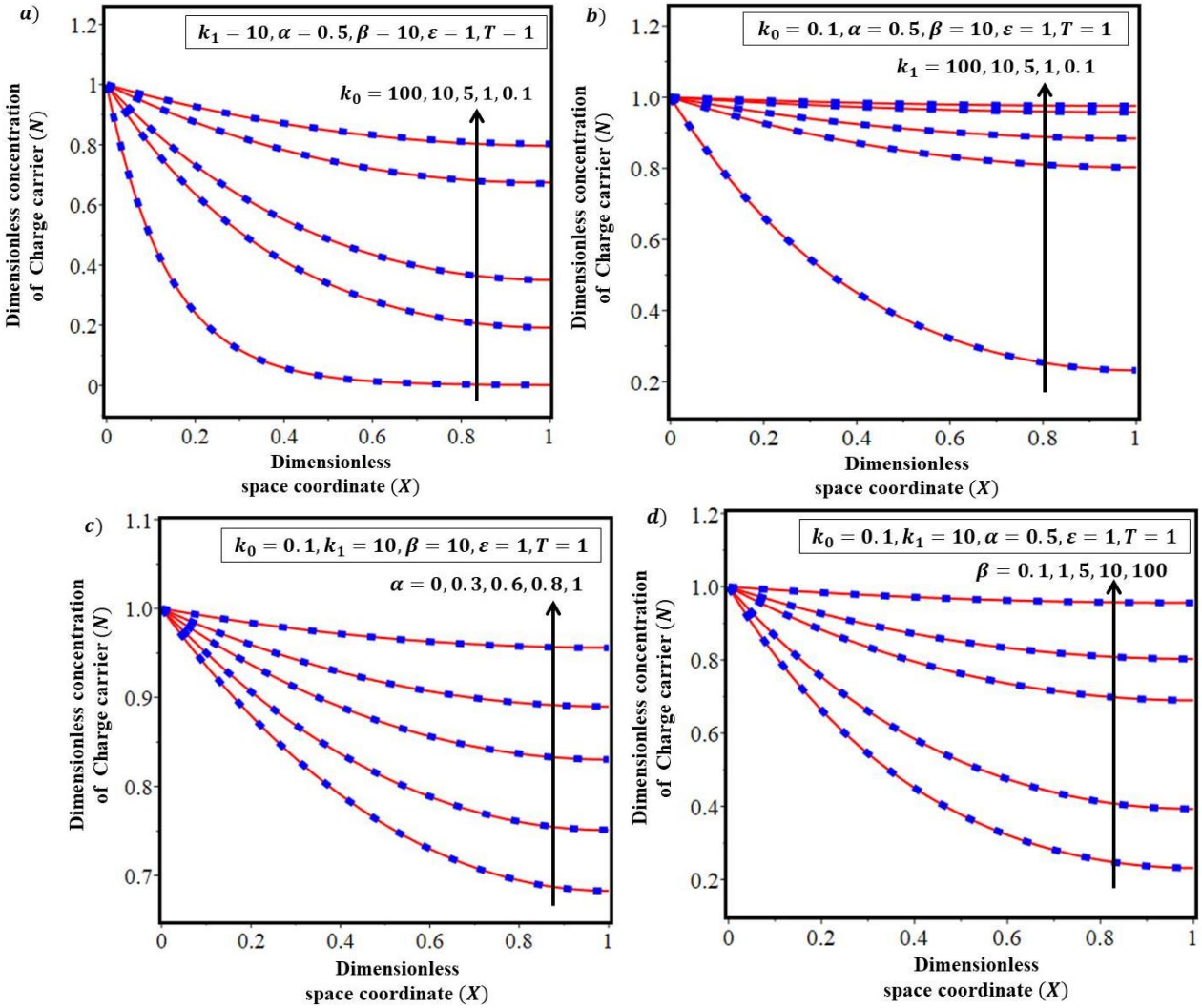

Figure S3. Comparison between analytical (dotted) and numerical (solid) results for the dimensionless concentration of charge carrier (N) against the dimensionless space coordinate (X) for various values of the parameters (Eq. (26)).